

Elementary excitations in modulation-doped Cd(Mn)Te quantum wells

Bernard Jusserand

Concepts and Devices for Photonics, FTR&D-CNRS, 196 Avenue Henri Ravera, 92225 Bagneux Cedex, France

Grzegorz Karczewski, Grzegorz Cywiński, and Tomasz Wojtowicz

Institute of Physics, Polish Academy of Sciences, Aleja Lotników 32/46, 02-668 Warszawa, Poland

Aristide Lemaître, Christophe Testelin, and Claudette Rigaux

Groupe de Physique des Solides, Universités Paris 6 et 7, 2 Place Jussieu, 75251 Paris Cedex 05, France

(Received 16 November 2000; published 3 April 2001)

We report on the observation of dispersive elementary excitations of two-dimensional electron gases in modulation-doped CdTe and $\text{Cd}_{1-x}\text{Mn}_x\text{Te}$ quantum wells. From the plasmon dispersion, we deduce electron densities in good agreement with the ones deduced from independent experiments, provided that a finite lifetime of the electron-hole pairs is taken into account within a modified random phase approximation model. We also find in the same samples uncorrelated electron-hole excitations at energies significantly lower than expected from the electron density. We discuss the possible implications of these findings in terms of electron localization.

DOI: 10.1103/PhysRevB.63.161302

PACS number(s): 73.63.Hs

The physics of elementary excitations of low-dimensional electron gases has been intensively studied in the past 20 years, mostly in the model system of modulation-doped quantum wells.¹ This system provides a unique configuration of high mobility electrons with a tunable density and a metallic behavior down to very low temperatures. The predictions of the random-phase approximation (RPA) has been extensively investigated and provide a very good description of numerous experimental results, mostly obtained in GaAs/Ga_{1-x}Al_xAs heterostructures. In this high purity system, scattering due to remote doping atoms and residual impurities are so small that the lifetime of electron-hole pairs close to the Fermi energy can be safely considered as infinite while, on the other hand, exchange-correlation effects generally play a minor role. Electron gases in modulation-doped quantum wells based on II-VI materials, such as CdTe, offers a new situation because larger values of r_s are more easily accessible due to the smaller Bohr radius [$\pi n(r_s a_B)^2 = 1$, where n is the two-dimensional electron density and a_B is the Bohr radius, equal to 6 nm in CdTe instead of 10 nm in GaAs]. Corrections due to collective interactions are expected to become more important.^{2,3} Thanks to the significant recent advances⁴ in the epitaxy of modulation-doped II-VI heterostructures and despite the fact that they still have not reached a quality comparable to the GaAs ones, it is therefore of great interest to investigate the spectrum of their elementary excitations. In this paper, we report on the observation by inelastic light-scattering experiments of elementary excitations of free-electron gases in CdTe and $\text{Cd}_{1-x}\text{Mn}_x\text{Te}$ quantum wells. We report also significant differences between the measured dispersions and standard RPA predictions. Our results are discussed in terms of defects scattering and electron-electron interactions.

Inelastic light scattering is a well-established method to investigate the elementary excitations of electron gases in semiconductors.^{1,5,6} Because of the wave vector conservation, one can measure the dispersion of elementary excita-

tions in the range $0-2 \times 10^5 \text{ cm}^{-1}$ typically, by simply tilting the sample with respect to the incident direction of light. Thanks to distinct polarization selection rules, plasmons, uncorrelated electron-hole pair excitations (the so-called single particle excitations, SPE), and spin-density excitations can be reliably identified. Moreover, as we have demonstrated recently on a GaAs modulation-doped quantum well,⁷ the plasmons and the SPE display mutually exclusive resonances at different virtual interband transitions. This further reinforces their identification. Based on these properties, we have identified in the inelastic light-scattering spectra on both CdTe and $\text{Cd}_{1-x}\text{Mn}_x\text{Te}$ structures the following features: (a) a plasmon line, with a well-defined dispersion which cannot be correctly described with the standard two-dimensional square-root dependence on the in-plane wave vector, contrary to what applies generally in GaAs structures; (b) a low-energy line with a linear dispersion, which displays the specific features typical of single-particle excitations in GaAs, with significant departures however.

We have studied two different series of samples, each containing a single quantum well made of either CdTe (series Cd) or $\text{Cd}_x\text{Mn}_{1-x}\text{Te}$ (series Mn), respectively.⁴ In all samples, the well is 10 nm thick, the barriers are made of $\text{Cd}_x\text{Mn}_{1-x}\text{Te}$ with 15% of Mg and modulation doping is obtained from iodine atoms inserted within the top barrier only. In the CdTe series, we compare three different samples, identical except for the thickness of the spacer layer which amounts to 20, 40, and 60 nm in samples Cd20, Cd40, and Cd60, respectively. In the $\text{Cd}_{1-x}\text{Mn}_x\text{Te}$ series, we compare two samples identical except for the Mn concentration in the quantum well (1.8% in Mn18 and 2.1% in Mn21). The spacer thickness is 40 nm. The Mn series is made of semi-magnetic compounds and displays specific behaviors under small applied magnetic fields. In this paper, we focus on Raman results at vanishing field and the two series of samples are expected to behave similarly except for an increased disorder due to alloy scattering in the Mn series.

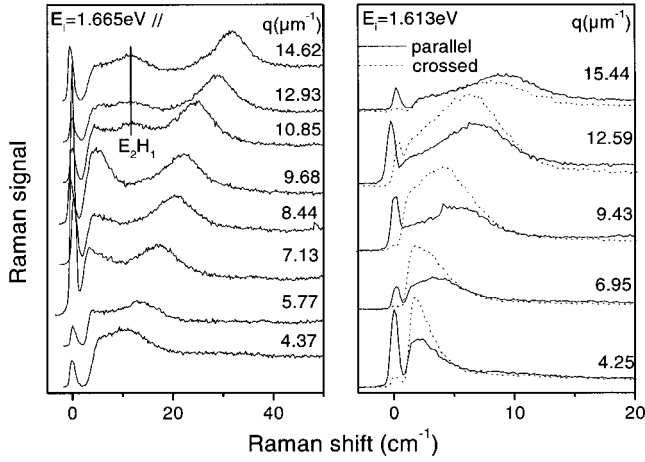


FIG. 1. Resonant inelastic light-scattering spectra on Cd20 sample shown as a function of the in-plane wave vector transferred to the electron gas for two different incident laser energies. For $E_i=1.665$ eV (left) and for $E_i=1.613$ eV (right), the signal due plasmons (respectively, SPE) is strongly enhanced due to selective resonances.

Raman data have been taken on samples immersed in superfluid helium ($T=1.8$ K), using a Ti-sapphire laser with a typical incident power density of 10 W/cm².

We show in Fig. 1(a) the wave-vector dependence of Raman spectra obtained on sample Cd20, with an incident laser energy close to the zone-center E_2H_1 excitonic transition associated with the second (empty) conduction subband. Such an incident energy provides selective resonances for plasmons.⁷ In this sample as well as in all others, a single Raman line is observed in these conditions and displays a strong parallel polarization. We assign this line to the plasmon excitation of the electron gas. We show in Fig. 1(b) the wave-vector dependence of a second Raman line which comes to resonance, when the laser energy is close to the E_1H_1 direct transition at the Fermi wave vector k_F , a distinctive character of SPE.⁷ This Raman line is observed in both polarizations with comparable magnitudes. A similar structure is observed in the other samples, but its energy strongly decreases when going from Cd20 to Cd60 and becomes very small in the Mn samples. Based on these properties, we tentatively assign this line to single-particle excitations. To summarize, the electronic Raman spectra of II-VI compounds, reported in this paper for the first time, to the best of our knowledge, look qualitatively similar to the one in GaAs quantum wells, despite of the significantly lower electron mobility. When comparing the measured dispersions to the RPA predictions, one must however, realize that strong departures appear, which have never been reported for GaAs structures.

We show in Fig. 2 the measured dispersion of the different Raman lines observed in the five different samples and we compare them with standard theoretical predictions. RPA predicts for the plasmon a square-root dependence on the in-plane wave vector, with a vanishing energy at vanishing q :⁸

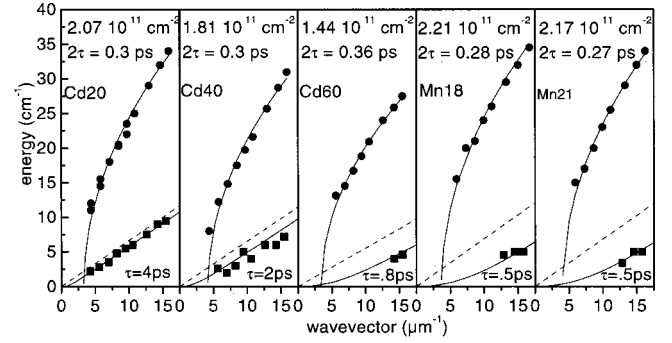


FIG. 2. Comparison between the dispersions measured in the five samples (plasmons, full dots; SPE, full squares) and the ones calculated according to different models discussed in the text [Eq. (2) in dashed line and Eq. 4 in full line for SPE; Eq. (3) in full line for plasmons].

$$\omega_P = \left(\frac{ne^2q}{2\epsilon m^*} \right)^{1/2}, \quad (1)$$

where ϵ is the background dielectric constant and m^* is the effective mass at the Fermi wave vector k_F . This mass is usually taken as the bare effective mass, eventually taking into account nonparabolicity corrections at k_F but neglecting additional corrections due to electron-electron interactions. The ‘‘cyclotron mass’’ generally gives a good estimation of the relevant quantity.

On the other hand, the SPE line is expected to vanish at vanishing wave vector and to display a linear dispersion with a slope equal to the Fermi velocity v_F :

$$\omega_{\text{SPE}} = v_F q = \hbar k_F q / m^* = \hbar \frac{\sqrt{2\pi n}}{m^*} q. \quad (2)$$

The measured plasmon dispersion does not display any distinctive square-root dispersion [Eq. (1)]. Assuming a linear dispersion, and a SPE character for the line, and in spite of the distinctive plasmon selection rules and resonance, the deduced electron density would be of the order of 2.0×10^{12} cm⁻², ten times more than the density expected from the parameters of the sample. We thus reject this tentative assignment and reexamine the plasmon behavior. Following Ref. 9, we include a finite lifetime of the electron-hole pairs within the RPA calculation.

In Ref. 9, a perturbative treatment of the diffusion of electron-hole pairs caused by the scattering on defects is introduced, which assumes a δ -function electron-defect interaction and a finite lifetime τ for the electron-hole pairs. A plasmon dispersion is deduced for $T=0$ K, which reduces to

$$\omega_P = \left(\frac{v_F^2 q \kappa}{2} - \frac{1}{4\tau^2} \right)^{1/2} \quad (3)$$

when q is sufficiently small as compared to the Thomas-Fermi screening wave vector $\kappa = e^2 m^* / 2\pi \hbar^2 \epsilon$. The plasmon oscillations are predicted to soften strongly at small wave vector and they only exist for wave vectors larger than a critical value. The corresponding ‘‘shifted square-root’’ dis-

TABLE I. Experimental information on the electron gases deduced from our Raman scattering and luminescence data and from magneto-transmission measurements (Ref. 2).

		Cd20	Cd40	Cd60	Mn18	Mn21
Luminescence	E_F (meV)	5	3	2	4	4
	n (10^{11} cm^{-2})	2.2	1.3	0.9	1.8	1.8
Magneto-transmission	n (10^{11} cm^{-2})		1.95		2.25	2.25
Plasmons	n (10^{11} cm^{-2})	2.07	1.81	1.5	2.4	2.2
	2τ (ps)	0.31	0.30	0.36	0.27	0.28
	$\hbar/2\tau$ (cm^{-1})	17	17	14	20	18.5
	FWHM (cm^{-1})	8.1	5.2	4.2	8.6	8.0
SPE	τ (ps)	4	2	0.8	0.5	0.5

persion gives an excellent description of our experimental findings. This experiment on Cd(Mn)Te modulation-doped quantum wells is the first clear observation, to the best of our knowledge, of a finite lifetime effect on the plasmon dispersion. The same model also predicts a finite ‘‘lifetime width’’ for the plasmon line, which is equal to $1/2\tau$. We report in Table I the values of the electron density (using a ‘‘cyclotron mass’’ of 0.105 and a background dielectric constant of 10) and the lifetime of the electron-hole pairs deduced from the fit of the plasmon dispersion. We also give the full width at half maximum (FWHM) of the plasmon line. Concerning the fitted densities, our data confirm that the transferred electron density decreases systematically when the thickness of the spacer layer is increased. The values of n obtained for Cd20 and the Mn samples are in excellent agreement with the values deduced from the Landau-level depopulation measured in magnetotransmission experiments on the same samples.² The agreement with the rough estimations deduced from the width of the luminescence line, taken with similar illumination conditions, is good, except for Cd40 and Cd60. We show in Fig. 3 the normalized luminescence lines for the five samples. In modulation-doped quantum wells, the luminescence extends over a finite range of energies corresponding to the recombination between doping electrons within the whole Fermi sea and a photocreated hole, relaxed at the top of the valence band. The width of the luminescence line thus provides a measure of the Fermi energy. The accuracy of this

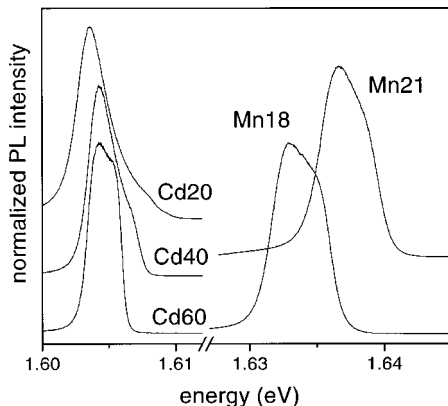


FIG. 3. Normalized luminescence spectra on the five samples.

measure is low, because of the uncertainties in the position of the gap E_0 and the Fermi edge E_F within the luminescence line. Concerning the lifetimes on the other hand, the values fitted from the plasmon dispersion are very small and of similar magnitudes for all samples. The corresponding ‘‘lifetime widths’’ are at least twice larger than the measured plasmon FWHM though the variations from sample to sample display consistent trends. We will discuss these points further below.

Concerning the SPE dispersion, a correct description of the experimental results based on Eq. (2) and the electron density deduced from the plasmon dispersion can be obtained for Cd20 only. We report in Fig. 2 the peak positions, measured as a function of the angle of incidence. These positions decrease with decreasing q . Below 2.5 cm^{-1} , they become too close to the elastic scattering at the laser energy to be accurately determined. In samples Cd20 and Cd40, the measurements extend over a sufficient range of the wave vector to prove the linear character of the dispersion. In Cd20, the slope agrees well within experimental accuracy with the value deduced from the density, assuming a standard degenerate electron gas. In Cd40, an anomalous decrease of the peak frequencies is observed but the slope remains fairly consistent with the plasmon measurement. In Cd60, Mn18, and Mn21, the low-energy lines are only detectable at large q and the slopes can no longer be determined. The experimental anomaly, already present in Cd40, becomes very strong: the SPE energies are much smaller than expected from the value of the electron density deduced from the plasmon dispersion (dashed lines in Fig. 2). The origin of these unexpected features is not yet fully understood. They are likely to reflect the unusually short lifetime of the electron-hole pairs, as deduced from the plasmon dispersion. We show in Fig. 2 the dispersion of the peak SPE energies calculated using the response function of the noninteracting electron gas, as given in Ref. 9:

$$\chi_0(\omega, q) \propto \frac{\omega}{\sqrt{(\omega + i/\tau)^2 - v_F^2 q^2} - i/\tau} - 1. \quad (4)$$

This expression was derived using some strong approximations but we have preferred to use it rather than the Lindhard-Mermin formula^{1,5} to be consistent with the plasmon analysis. Using the densities deduced from the plasmon dispersion, we cannot fit the SPE data with the very short plasmon lifetimes but with much larger values, significantly varying from sample to sample (see Table I). This fit is not very conclusive for Cd60, Mn18, and Mn21, because of the limited experimental information but we think that a significant decrease of the lifetime in these samples is demonstrated and the estimated values are given in Table I.

Let us now compare the experimental information which we have deduced on the disorder effect in our samples from the plasmon and SPE dispersions and from the luminescence line shapes. Contrary to the electron density, which is consistently deduced from the different observations, when available, the lifetime determinations show some discrepancies. According to the fit of the plasmon dispersion, disorder effects, due to impurities or alloy fluctuations, should not

vary significantly from sample to sample, in clear contradiction to the strong trends observed for the SPE dispersion and the luminescence lineshape. It is now well established^{10,11} that the activation in the luminescence line of non-vertical recombinations between occupied conduction electrons with finite wave vector and photocreated holes relaxed in near-zone center valence states is due to potential fluctuations. Depending on the amplitude of these fluctuations, the luminescence line shape either peaks at the zone-center band gap, for instance, in high-quality GaAs quantum wells,¹⁰ or extends up to the Fermi-edge energy without significantly decreasing, for instance, in quantum wells made of $\text{In}_{1-x}\text{Ga}_x\text{As}$ alloys.¹¹ In our Mn samples, the second behavior is observed (see Fig. 3) and clearly reflects alloy disorder due to the substitution of Cd atoms by Mn ones. In Cd samples, the line shape evolves from a peaked structure in Cd20 towards a broad one in Cd60. As significant variations of the disorder are not expected in these samples, which are very similar except for the spacer layer thickness, we attribute this continuous evolution to the decreasing electron density and the increasing sensitivity of conduction electrons to potential fluctuations. The Raman observations associated to the SPE lines are fully consistent with this analysis: the departure from a pure degenerate behavior is large in the Mn samples and increases continuously along the Cd series. This behavior is not corroborated by our analysis of the plasmon dispersion, which indeed shows a strong departure from the ideal dispersion in high mobility electron gas but also exhibits very small variations from sample to sample and gives inconsistent values for the lifetime τ and the linewidth. This likely reflects that the perturbative treatment of impurity scattering introduced in Ref. 9 is insufficient to reproduce quantitatively the experimental departures from the standard behavior reported in this paper.

To conclude, we have reported the first observation, to the best of our knowledge, of the low-energy excitations of a two-dimension electron gas embedded in modulation doped

Cd(Mn)Te single quantum wells. While the overall trends follow the standard picture established on GaAs wells, significant quantitative departures appear, which we have analyzed in terms of disorder induced finite lifetimes of the electron-hole pairs across the Fermi energy. In low-density GaAs heterostructures, a transition has been observed in the luminescence spectrum¹² which is dominated by band electrons at large densities and becomes dominated by charged excitons when the density is decreased. This transition is correlated to a strong drop in the conductance of the sample and has been attributed to a metal-insulator transition.¹² Localization of electrons has been directly demonstrated by near-field spectroscopy in the same regime.¹³ The luminescence properties of electron gases in II-VI quantum wells display the same transition at densities slightly smaller than available in our samples.^{3,14} Even though conductance measurements have not been yet reported, a localization transition is thus very likely to exist in II-VI quantum wells. Above but close to this transition one should certainly expect strong departures from the standard degenerate electron gas behavior such as the ones reported in this paper. Fundamental questions about (i) the type of states (localized or extended) which are likely to contribute to the plasmon oscillation, (ii) the effective mass of the electron-hole pairs when the Fermi edge is above but close to the mobility edge, and finally (iii) the necessary modifications to the many-body corrections at k_F due to disorder, have not been yet considered in detail from the theoretical point of view. We expect that the detailed experimental results reported in this work will help to develop such a theory.

We acknowledge F. Laruelle, J. Cibert, V. Huard, R. Cox, K. Saminayadar, D. Richards, and F. Perez for very helpful discussions and valuable comments on the manuscript. We also acknowledge the State Committee for Scientific Research Poland for the support through Grants Nos. PBZ 28.11/P8 and 2-P03B 119 14.

¹A. Pinczuk and G. Abstreiter, in *Light Scattering in Solids V*, edited by M. Cardona and G. Güntherodt (Springer-Verlag, Berlin, 1989), p. 153.

²A. Lemaître, C. Testelin, C. Rigaux, T. Wojtowicz, and G. Karczewski, *Phys. Rev. B* **62**, 5059 (2000).

³V. Huard, R. T. Cox, K. Saminayadar, A. Arnoult, and S. Tatarenko, *Phys. Rev. Lett.* **84**, 187 (2000).

⁴G. Karczewski, J. Jaroszynski, A. Barcz, M. Kutrowski, T. Wojtowicz, and J. Kossut, *J. Cryst. Growth* **184/185**, 814 (1998).

⁵G. Fasol, R. D. King-Smith, D. Richards, U. Ekenberg, N. Mestres, and K. Ploog, *Phys. Rev. B* **39**, 12 695 (1989).

⁶B. Jusserand, H. Peric, D. Richards, and B. Etienne, *Phys. Scr.* **T49**, 503 (1993).

⁷B. Jusserand, M. N. Vijayaraghavan, F. Laruelle, A. Cavanna,

and B. Etienne, *Phys. Rev. Lett.* **85**, 5400 (2000).

⁸F. Stern, *Phys. Rev. Lett.* **18**, 546 (1967).

⁹G. F. Giuliani and J. J. Quinn, *Phys. Rev. B* **29**, 2321 (1984).

¹⁰H. Peric, B. Jusserand, D. R. Richards, and B. Etienne, *Phys. Rev. B* **47**, 12 722 (1993), and references therein.

¹¹M. S. Skolnick, J. M. Rorison, K. J. Nash, D. J. Mowbray, P. R. Tapster, S. J. Bass, and A. D. Pitt, *Phys. Rev. Lett.* **58**, 2130 (1987).

¹²G. Finkelstein, H. Shtrikman, and I. Bar-Joseph, *Phys. Rev. Lett.* **74**, 976 (1995).

¹³G. Eytan, Y. Yayon, M. Rappaport, H. Shtrikman, and I. Bar-Joseph, *Phys. Rev. Lett.* **81**, 1666 (1998).

¹⁴K. Kheng, R. T. Cox, Y. Merle d'Aubigné, F. Bassani, K. Saminayadar, and S. Tatarenko, *Phys. Rev. Lett.* **71**, 1752 (1993).